Presolidification in Eutectic Droplets

Bene Poelsema, Zhiguo Zhang, Harold J. W. Zandvliet, and Arie van Houselt*
Physics of Interfaces and Nanomaterials, MESA+ Institute for Nanotechnology, University of Twente, P.O. Box 217, 7500 AE Enschede, Netherlands

(Received 16 November 2022; revised 31 July 2023; accepted 3 August 2023; published 8 September 2023)

Evidence of presolidification, the counterpart to premelting, is reported. Near the eutectic temperature, T_C, the propagation direction of thermal gradient driven motion of eutectic Ge-Pt droplets on Ge(110) is determined by presolidification. Well above T_C, the micron-sized droplets move towards the hottest location at the substrate, irrespective of crystalline direction. At 90 K above T_C, a strong, unanticipated preference for propagation along the substrate [001] azimuth suddenly emerges, which is attributed to presolidification at the liquid-solid interface. The propagation along [001] is accompanied by a distinct change in shape from compact to elongated along [001].

DOI: 10.1103/PhysRevLett.131.106201

Introduction.—Premelting—the loss of crystallinity before the bulk material melts—is well documented (e.g., [1,2]). For instance, for pure Pb(100) premelting starts already at ∼40 K below the melting temperature. Presolidification, the counterpart to premelting, has received, however, much less attention. Here we report presolidification in eutectic droplets at no less than 90 K above the eutectic temperature T_C.

The dynamics of metal containing eutectic droplets on semiconductor surfaces has received considerable attention. This includes thermomigration of PtSi [3–5], of AuSi and AuGe droplets [6–8], electromigration of AuGe [9], and the motion of Ga droplets on GaAs under incongruent evaporation conditions [10,11]. The surface studies were motivated by interest in possibilities for bottom-up fabrication of nanostructures, catalysis of standing up [12] and lying down nanowires [13–19] on surfaces, and by genuine interest in the complex physics of the motion of metallic droplets on surfaces.

The eutectic droplets move under influence of a temperature gradient. The gain of entropy is the driving force for the motion of the droplets towards the location at the highest temperature (e.g., [20]). During their motion the droplets stay at the high-host-content liquidus line, in thermal equilibrium with the substrate (see Refs. [21,22] for the Ge-Pt phase diagram). A tendency for droplets to follow a step-up route has been suggested [6,7,9,23]. Motion along a specific crystalline direction has not yet been reported for a closed (mass conserved) system as studied here, but was found for Au-Si eutectic droplets along Si[1-10] on Si(110) during continuous deposition of Au [24].

We have recently studied the motion of micron-sized Ge-Pt eutectic droplets on Ge(110) [20,25]. At a temperature of ∼50 K above T_C we observed that the droplets travel radially toward the temperature maximum at (or near) the center of the substrate. Occasionally, some guidance along major step bunches was found. The classic Cline and Anthony concept of dissolution-diffusion-redeposition for bulk diffusion [26], with diffusion of host material through the eutectic droplet as the rate limiting step, does not apply for this surface migration [20]. Upon solidification, complex crystalline features emerge after spinodal decomposition [27]. In our current contribution we investigate the motion of micron-sized Ge-Pt eutectic droplets in relatively low Pt content regions, ∼4 mm from the hottest spot at the substrate. We focus on the influence of the surface temperature from ∼110 K above T_C to just below T_C ($T_C = 1050$ K). In line with Ref. [20], we confirm that the velocity can be described with an activation energy of about 2–2.5 eV, which we attributed before to dissolution of the wetting layer at the leading edge of the compact droplet as the rate limiting step. We find at about 1140 K a totally unanticipated change of direction by 40° and a concomitant shape change from compact to elongated. This is attributed to presolidification of the droplet at its interface with the substrate.

Results.—We have prepared a Pt containing Ge(110) surface by deposition of a few monolayer equivalents at room temperature. The system was subsequently heated slowly to ∼110 K beyond T_C. Figure 1 shows a number of frames taken from a photoemission electron microscopy (PEEM) movie. The white blobs represent eutectic droplets. Droplets with a diameter of about 4 microns or less remain sessile and stable in line with earlier observations [20]. Initially, the larger droplets move at a velocity of roughly 600 nm/s. The figure shows centers of mass (x, y) positions of six droplets, marked cyan, red, blue, yellow, orange, and pink, that initially move roughly horizontally from left to right. The observations affirm our earlier observations for the same system and that behavior is well understood [20,25,27]: The eutectic droplets move under

the influence of a thermal gradient towards the hottest location at the surface. They do so irrespective of step patterns or crystallographic preferences [20]. Only in the vicinity of multistep bunches the isotropy in the traveling direction is reduced locally. The traveling speed is slightly higher for particles that move along a previously formed trail, as is the case here. Currently, we focus on "Pt-poor" (see further in the Letter) locations at the surface at ∼4 mm distance from the hottest spot. We follow six droplets, first traveling in goose step along a preformed trail. Initially, the set of droplets moves at the same speed and in the same direction. We have identified earlier the gain in entropy of a droplet with increasing temperature as the driving force for its motion towards a warmer location. This conclusion becomes immediately obvious if we consider Maxwell's equation for the Gibbs free energy, $dG = -SdT + VdP$. For a fixed number of particles at constant pressure, as is the case here, we find thus that the lowest Gibbs free energy is reached at the highest temperature. The magnitude of dG/dT is given by the absolute value of the entropy S. The magnitude of S increases with T and this driving force is for the eutectic PtGe droplets even enhanced, since the travel of a eutectic droplet towards higher temperature, along the Ge-rich liquidus line in the phase diagram, leads to more Ge atoms originating from the substrate becoming part of the liquid droplet. Figure 2 shows data for the droplets marked with the corresponding colors in Fig. 1. The droplets are subjected to a temperature variation as indicated by the continuous red curves. Initially, the droplets move about horizontally toward the hottest spot at the surface. Surprisingly, the propagation direction changes suddenly and drastically by about 40° when the falling temperature passes 1140 K and further remains constant upon cooling (this directional motion is indicated by the gray zones in Fig. 2). The specific azimuth is defined as the [001] direction on Ge(110) after a careful analysis of the relationship with the diffraction pattern for the relevant field of view [28]. A subsequent rise of the temperature leads to a sudden opposite change of the propagation direction, again at 1140 K. The unanticipated change of propagation direction is thus fully reversible as confirmed by another subsequent drop in the temperature. The traveling speed of the droplets is monitored continuously and the result is shown in Fig. 2(b). Upon dropping the temperature from 1160 to 1060 K the traveling speed of the droplets decreases continuously from ∼600 to ∼20 nm/s. The traveling speed of a droplet through the (2 × 1) wetting layer has been analyzed previously and explained [20]. In short (more details in [21]): the dissolution of the wetting layer at the advancing edge of the droplet was identified as the speed limiting factor with an activation energy of ∼2.2 eV per edge atom. The marked and irregular variation of the propagation speed is by no means accidental and each individual speed-drop can be traced back to interactions with either one or more neighboring clusters or passage through less homogeneous areas; see Ref. [21].

Another eye catching observation is that the compact-shaped eutectic droplets assume an elongated shape when traveling along [001], i.e., for temperatures below 1140 K. The aspect ratio increases with decreasing temperature until solidification takes place at the eutectic temperature of 1050 K. The corresponding data are exhibited in Fig. 3. The length to width (aspect) ratio has been taken from snapshots

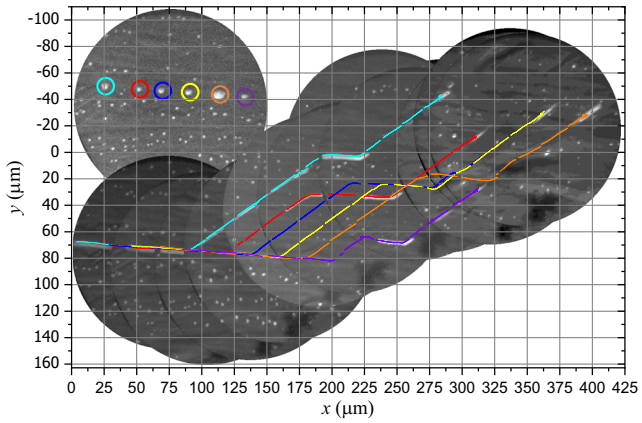

FIG. 1. Snapshots from a PEEM movie (field of view 150 micron, 4.9 eV photons) of Ge-Pt droplets [21]. The straight-line segments illustrate the evolution of the positions of the center of gravity, coordinates (x, y) in microns, of the eutectic droplets marked by colored circles in the image in the top-left. The white points are smaller droplets (diameter < 4 μm), which are immobile. Their positions are used to calibrate the translational motion of the surface underneath the objective. Above T_C, the larger droplets move towards the highest temperature spot. The experimental system is carried through a temperature trajectory that is specified in Fig. 2. At $x = 190$ μm the cyan droplet is hindered by an immobile one and at $x = 310$ μm the blue and yellow droplets merge and continue as a new entity.

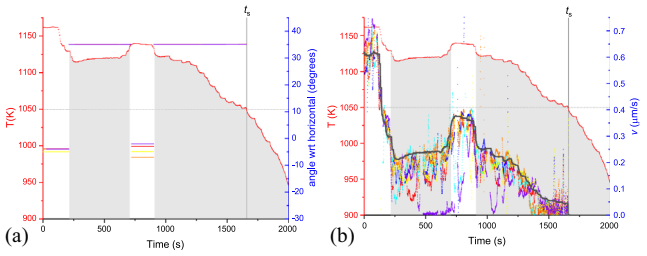

FIG. 2. Panel (a) shows the actual propagation direction of the encircled droplets in Fig. 1 (the colors correspond) with an uncertainty of ∼1° (right y axis). The red curves in both (a) and (b) exhibit the temporal variation of the temperature (left y axis). The gray shadow represents the motion along the [001] direction on Ge(001). Panel (b) shows the migration speed of the droplet's center of gravity (right y axis), see text. The black curve represents the speed calculated with an Arrhenius expression and activation energy of 2.5 eV (see text). The vertical line denoted with t_s marks the solidification of the droplets at T_C. No mobility is observed below T_C.

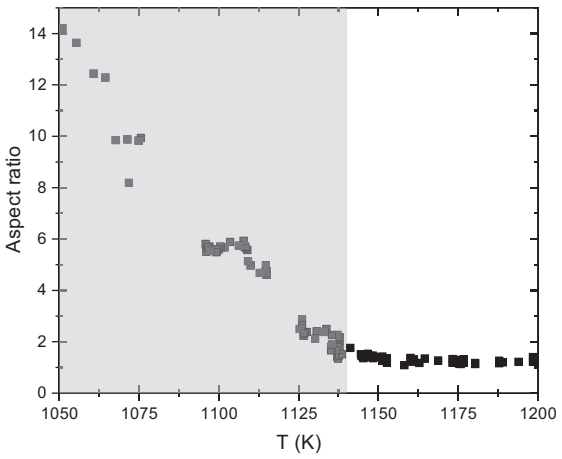

FIG. 3. Aspect ratio (length or width) of a moving droplet as a function of temperature. Globally the time runs from right to left, but the temperature profile is quite complex. Between ca. 1075 and 1110 K the droplet moves through a heterogeneous area, compromising the shape of the droplet. The corresponding data points have been left out since they are not characteristic for motion through the (2×1) wetting layer. For a similar reason (huge length of the droplet and thus surface inhomogeneities) large values the lowest temperature data are less exact and must be taken with care. In the gray shaded part of the graph the droplets moved in the [001] direction.

of a mirror image type LEEM movie [21]. Most data points are extracted for the droplets that travel through the (2×1) wetting layer (see Ref. [20]). Heterogeneity compromises the width and length of the droplet. (Compare for instance movie 2 in [21] between $t = 9{:}56{:}30$ and $9{:}58{:}15$). As mentioned before, the heterogeneity is attributed to the exchange of Ge atoms between the droplet and the substrate, probably in a previous experiment. As evident from the movie, the width of the elongated droplets gets constricted when it passes the heterogeneous area, with consequences for the length too. Once more it is stressed that the results have been obtained irrespective of the history, i.e., the transition between compact and elongated droplets and vice versa were observed repeatedly both when passing the critical temperature of 1140 K during the increase and decrease of the substrate temperature. We consider this as strong evidence that equilibrium physics governs the shape and propagation direction of the droplets. The higher speeds [cf. Fig. 2(b)] are representative for unperturbed motion through the (2×1) wetting layer. It therefore makes sense to compare these to the results calculated with an Arrhenius expression with activation energy of E for dissolution of an edge atom [20]. The result for $E = 2.5$ eV is represented by the black curve in Fig. 2(b) and we find a decent agreement over the entire temperature range showing that the propagation speed does not depend on the compactness of the droplet, neither on the direction of motion, suggesting an identical rate

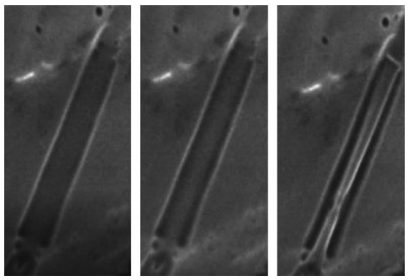

FIG. 4. Snapshot from a LEEM mirror mode movie [21], area 12×26 μm^2, start voltage -1.3 eV. The panels show an elongated droplet during cooling at a rate of 0.3 K s^{-1} through the eutectic transition, which starts in the central panel and has completed in the right hand one. The time difference between the panels is starting from left, respectively, 4 and 1 s. The homogeneous central part of the images represents the (2×1) wetting layer, while the heterogeneity in the bottom and top areas is due to ejected Ge from earlier experiments (see text).

limiting step as expected within this view and thus reconfirms its correctness (see further [21] paragraph S6).

For completeness we show in Fig. 4 parts of snapshots of a LEEM movie [21] that demonstrate the fast transition from droplet to solid when passing through T_C. The brighter edges are attributed to local field distortion typical in LEEM/PEEM from rough surfaces, allowing a relatively accurate determination of the data displayed in Fig. 3. The darker inside in the first panel reflects a lower work function of the eutectic liquid compared to the surrounding (2×1) environment of the wetting layer. Upon passage of T_C not less than 1.59 Ge-atoms per involved Pt-atom are instantaneously ejected during the spinodal decomposition. They most probably bind to the Ge substrate along the edges. The darkness of the outer skirts of the elongated feature is attributed to a lower work function due to the resulting rough local morphology. Below T_C all Pt atoms are incorporated into a Ge_2Pt crystallite in the center with a higher work function and thus a brighter appearance, cf. the third panel. The second panel illustrates the process during the fast transition. We therefore utilize this *in vivo* visualization of the spinodal decomposition as a powerful way to calibrate the temperature scale within 0.3 K, assuming that it agrees with the bulk phase diagram. The constriction at about $\frac{1}{4}$ of the bottom is due to coalescence of crystallites that nucleated on, and grew from, the top and the bottom (see movie). We finally note that we could not detect any mobility of Ge or Ge-Pt features below T_C. This observation is attributed to the loss of entropy during solidification and thus of driving force on Ge-Pt clusters to move towards locations at higher temperature.

Discussion and conclusion.—Our current findings demonstrate presolidification. For pure (elemental) liquids presolidification during approach of the melting temperature has not been reported. In thin films layering near the liquid-solid interface above the melting temperature has

been observed [29], sometimes with epitaxially induced surface parallel order [30]. Interestingly, surface crystallization at the vacuum-liquid interface of the AuSi alloy has been revealed by GIXD, Grazing incidence x-ray diffraction, at 11 K above T_C [31]. For the current liquid GePt alloy, we do not find evidence for presolidification at the vacuum interface. However, for the experimentally unfortunately not accessible liquid-solid substrate interface similar features appear an even more likely option, especially in the presence of favorable epitaxial conditions as is the case here. Under "poor Pt conditions" that apply for the data in Fig. 4 we previously found [27] that, just below T_C, orthorhombic $Ge_2Pt(101)$ crystallites emerge on Ge(110) with their b-axis parallel to Ge[001]. This alignment results from the minimal misfit between the b axis of $Ge_2Pt(101)$ and Ge[001]. The favorable epitaxial relationship at the liquid-substate interface renders presolidification a highly likely possibility for the eutectic GePt film on Ge(110). Presolidification thus provides a viable framework to explain our experimental observations. Up to 1140 K, that is 90 K above T_C, the elongation along [001] strongly increases with decreasing temperature (see Fig. 3). This is indeed attributed to presolidification, i.e., the layer of the Ge-Pt droplet in contact with Ge(110) already assumes the structure of $Ge_2Pt(101)$. For a solid two-dimensional heteroepitaxial island the geometrical shape results from the balance between strain relaxation and boundary energy. Since the edge energy along [001] is low due to the minimal misfit, the GePt feature elongates along this very azimuth. This agrees with the current finding shown in Fig. 3. On approaching T_C, the elongation increases which is attributed to enhanced ordering in the contact layer and the involvement of more layers in the droplet. The presolidification sets in surprisingly already at ~90 K above T_C. The overall composition of the droplet is governed by the position of the liquidus at any given temperature. The composition of the (ultimate layer of the) interface at the droplet side of the interface must, however, approach that of the Ge_2Pt solid. Above ~1140 K, the aspect ratio remains constant at 1.3. This consistent deviation from unity is attributed to residual orientational order in the PtGe liquid at the solid-liquid interface.

Within this framework we also explain the change in propagation direction from solely determined by the temperature gradient to exclusively along [001] below 1140 K. The presolidification aligns the contact layer in the droplet with Ge[001] with a very low misfit (~2%). Preferred travel along Ge[100] is attributed to reduced friction for touching layers when alignment occurs for the two touching layers [32,33]. Note that with increasing temperature the layering of the liquid at the interface becomes less pronounced and isotropic diffusion will prevail, in this case above 1140 K. The complexity of the motion of eutectic droplets on crystalline hosts is further reinforced by the recent findings of Curiotto *et al.* [24] for the system Au/Si(110). They reported that the Au-Si droplets move along Si[1–10] back and forth only under ongoing deposition of Au. Motion along an applied external electric field, irrespective of crystalline directions was also observed. Despite the seeming congeniality of the systems the motion of the eutectic Pt-Ge droplets on Ge(110) is completely different: it occurs spontaneously and is not inflicted by ongoing deposition of Pt, nor by applying an external electric field gradient. We suspect that anisotropic etching of host material at the droplet-host interface to fulfil and maintain the required Au-Si ratio in the eutectic is responsible for directionality in the Au/Si(110) system during deposition of gold [24]. We emphasize that the system under current investigation and similar eutectic systems are extremely complex due to severe mass exchange between the eutectic droplets and the substrate (or host). This is restricted to the host material but may well lead to transport of host material even over macroscopic (several mms) distances resulting in accumulation of deposited material (in our case Pt) near the hottest spot [20,25,27]. This surface area is referred to as "Pt-rich." During subsequent cooling, excess host material is expelled, which leads to severe local modifications of the morphology of the substrate [27]. The magnitude of these processes is extremely hard (even impossible) to quantify since they all depend on the deposited amount, the thermal profile and most strongly on thermal history. It is obvious, however, that the severeness of composition—and morphological modifications declines vastly with increasing distance from the hottest spot. The area we investigate currently can safely be judged as "Pt-poor" and, consequently, we consider the current findings as representative for the intrinsic behavior of eutectic Ge-Pt droplets on flat Ge(110). We summarize and conclude that well above T_C and in agreement with Ref. [20], we find that Pt-Ge eutectic droplets travel towards the hottest spot on the substrate. In the current case we concentrate on the motion of droplets in an area with a relatively low Pt content. Below about 1140 K the eutectic droplets move strictly along Ge[001]. At the same time, their originally compact shape undergoes a transition to an elongated one with its aspect ratio continuously increasing during cooling to T_C. Both observations are rationalized by presolidification in which (near) interface layers assume a $Ge_2Pt(101)$ lattice and align with their b-axis parallel to Ge[001]. This alignment was observed for the contact between the crystalline phases 90 K above T_C. The current findings for Ge-Pt eutectic droplets are explained using basic physics. Therefore, the observed increased elongation of the droplets upon approaching T_C is believed to generically prelude the later formation of "lying-down" nanowires, observed for a wide variety of systems: metals and rare earth metals on semiconductor surfaces.

Z. Z. thanks the China Scholarship Council (CSC 201708130089) for financial support. H. J. W. Z. and

A. v. H. acknowledge the Nederlandse organisatie voor Wetenschappelijk Onderzoek (NWO) for financial support.

B. P. and Z. Z. contributed equally to this work.

*A.vanHouselt@utwente.nl

[1] J. W. M. Frenken and J. F. van der Veen, Observation of Surface Melting, Phys. Rev. Lett. **54**, 134 (1985).
[2] B. Pluis, A. W. Denier van der Gon, J. W. M. Frenken, and J. F. van der Veen, Crystal-Face Dependence of Surface Melting, Phys. Rev. Lett. **59**, 2678 (1987).
[3] W.-C. Yang, H. Ade, and R. J. Nemanich, Stability and dynamics of Pt-Si liquid microdroplets on Si(001), Phys. Rev. B **69**, 045421 (2004).
[4] P. A. Bennett, J. Chobanian, J. I. Flege, E. Sutter, and P. Sutter, Surface thermomigration of nanoscale Pt-Si droplets on stepped Si(001), Phys. Rev. B **76**, 125410 (2007).
[5] P. Sutter, P. A. Bennett, J. I. Flege, and E. Sutter, Steering Liquid Pt-Si Nanodroplets on Si(100) by Interactions with Surface Steps, Phys. Rev. Lett. **99**, 125504 (2007).
[6] A. El-Barraj, S. Curiotto, F. Cheynis, P. Müller, and F. Leroy, Dynamics of Au-Ge liquid droplets on Ge(111) terraces: Nucleation, growth and dynamic coalescence, Appl. Surf. Sci. **509**, 144667 (2020).
[7] S. Curiotto, F. Leroy, F. Cheynis, and P. Müller, Surface-dependent scenarios for dissolution-driven motion of growing droplets, Sci. Rep. **7**, 902 (2017).
[8] B. H. Stenger, A. L. Dorsett, J. H. Miller, E. M. Russell, C. A. Gabris, and S. Chiang, Growth and motion of liquid alloy droplets of Au on Ge(110), Ultramicroscopy **183**, 72 (2017).
[9] F. Leroy, A. El Barraj, F. Cheynis, P. Müller, and S. Curiotto, Atomic Transport in Au-Ge Droplets: Brownian and Electromigration Dynamics, Phys. Rev. Lett. **123**, 176101 (2019).
[10] J. Tersoff, D. E. Jesson, and W. X. Tang, Running droplets of Gallium from evaporation of Gallium Arsenide, Science **324**, 236 (2009).
[11] J. Tersoff, D. E. Jesson, and W. X. Tang, Decomposition Controlled by Surface Morphology During Langmuir Evaporation of GaAs, Phys. Rev. Lett. **105**, 035702 (2010).
[12] S. Kodambaka, J. Tersoff, M. C. Reuter, and F. M. Ross, Germanium nanowire growth below the eutectic temperature, Science **316**, 729 (2007).
[13] O. Gürlü, O. A. O. Adam, H. J. W. Zandvliet, and B. Poelsema, Self-organized, one-dimensional Pt nanowires on Ge(001), Appl. Phys. Lett. **83**, 4610 (2003).
[14] H. J. W. Zandvliet, A. van Houselt, and B. Poelsema, Self-lacing atom chains, J. Phys. Condens. Matter **21**, 474207 (2009).
[15] C. Preinesberger, S. Vandré, T. Kalka, and M. Dähne-Prietsch, Formation of dysprosium silicide wires on Si (001), J. Phys. D **31**, L43 (1998).
[16] Y. Chen, D. A. A. Ohlberg, G. Medeiros-Ribeiro, Y. A. Chang, and R. S. Williams, Self-assembled growth of epitaxial erbium disilicide nanowires on silicon (001), Appl. Phys. Lett. **76**, 4004 (2000).
[17] N. Oncel and D. Nicholls, Iridium silicide nanowires on Si(001) surfaces, J. Phys. Condens. Matter **25**, 014010 (2013).
[18] H. W. Yeom, Y. K. Kim, E. Y. Lee, K. D. Ryang, and P. G. Kang, Robust One-Dimensional Metallic Band Structure of Silicide Nanowires, Phys. Rev. Lett. **95**, 205504 (2005).
[19] C. Zeng, P. R. C. Kent, T.-H. Kim, A.-P. Li, and H. H. Weitering, Charge-order fluctuations in one-dimensional silicides, Nat. Mater. **7**, 539 (2008).
[20] B. Poelsema, Z. Zhang, J. S. Solomon, H. J. W. Zandvliet, and A. van Houselt, Shining new light on the motion of eutectic droplets across surfaces: A PEEM study of PtGe on Ge(110), Phys. Rev. Mater. **5**, 125602 (2021).
[21] See Supplemental Material at http://link.aps.org/supplemental/10.1103/PhysRevLett.131.106201 for the movies from which the data in Figs. 1–3 are taken.
[22] J. S. Wang, S. Jin, W. J. Zhu, H. Q. Dong, X. M. Tao, H. S. Liu, and Z. P. Jin, First-principles calculations assisted thermodynamic assessment of the Pt-Ga-Ge ternary system, CALPHAD: Comput. Coupling Phase Diagrams Thermochem. **33**, 561 (2009).
[23] S. Curiotto, F. Leroy, F. Cheynis, and P. Müller, Self-propelled motion of Au-Si droplets on Si(111) mediated by monoatomic step dissolution, Surf. Sci. **632**, 1 (2015).
[24] S. Curiotto, F. Leroy, F. Cheynis, and P. Müller, In-plane Si nanowire growth mechanism in absence of external Si flux, Nano Lett. **15**, 4788 (2015).
[25] Z. Zhang, B. Poelsema, H. J. W. Zandvliet, and A. van Houselt, Detailed characterization of supported eutectic droplets using photoemission electron microscopy, Phys. Rev. Mater. **5**, 105601 (2021).
[26] H. E. Cline and T. R. Anthony, High-speed droplet migration in silicon, J. Appl. Phys. **47**, 2325 (1976).
[27] Z. Zhang, B. Poelsema, H. J. W. Zandvliet, and A. van Houselt, Microscopic study of the spinodal decomposition of supported eutectic droplets during cooling: PtGe/Ge {110}, J. Phys. Chem. C **126**, 11285 (2022).
[28] B. Poelsema, H. J. W. Zandvliet, and A. van Houselt, Stoichiometric edges during the intrinsic growth of hexagonal boron nitride on Ir(111), New. J. Phys. **21**, 092001 (2019).
[29] D. Kaminski, P. Poodt, E. Aret, N. Radenovic, and E. Vlieg, Observation of a Liquid Phase with an Orthorhombic Orientational Order, Phys. Rev. Lett. **96**, 056102 (2006).
[30] W. J. Huisman, J. F. Peters, M. J. Zwanenburg, S. A. de Vries, T. E. Derry, D. Abernathy, and J. F. van der Veen, Layering of a liquid metal in contact with a hard wall, Nature (London) **390**, 379 (1997).
[31] O. G. Shpyrko, R. Streitel, V. S. K. Balagurusamy, A. Y. Grigoriev, M. Deutsch, B. M. Ocko, M. Meron, B. Lin, and P. S. Pershan, Surface crystallization in a liquid AuSi alloy, Science **313**, 77 (2006).
[32] M. Dienwiebel, N. Pradeep, G. S. Verhoeven, J. W. M. Frenken, and H. W. Zandbergen, Model experiments of superlubricity of graphite, Surf. Sci. **576**, 197 (2005).
[33] M. Dienwiebel, G. S. Verhoeven, N. Pradeep, J. W. M. Frenken, J. A. Heimburg, and H. W. Zandbergen, Superlubricity of Graphite, Phys. Rev. Lett. **92**, 126101 (2004).